Remote forcing annihilates barrier layer in southeastern Arabian Sea

S. S. C. Shenoi, D. Shankar, and S. R. Shetye

National Institute of Oceanography, Goa, India.

Time-series measurements of temperature and salinity profiles were made every two hours at 74°30′E, 9°13′N in the southeastern Arabian Sea (SEAS) during 22-March–7-April and 23-May–7-June 2003 as part of the Arabian Sea Monsoon Experiment (ARMEX). The observations show that a 20 m thick barrier layer (BL) exists during March–April owing to a surface layer of low-salinity waters advected earlier during December–January from the Bay of Bengal. The BL is almost annihilated by 7 April owing to upwelling. The relic BL that survives is annihilated later in May by upwelling, and by the inflow of high-salinity waters from the north and by mixing due to stronger winds, which deepen the mixed layer. We present evidence from satellite data and arguments based on existing theories to show that both the upwelling and the advection of high-salinity waters are remotely forced.

Introduction

Remote forcing, especially from the Bay of Bengal (BoB), plays a major role in the dynamics of the southeastern Arabian Sea (SEAS) [*McCreary et al.*, 1993; *Shankar et al.*, 2002]. Remotely forced Kelvin and Rossby waves force the Lakshadweep High (LH), a high in sea level, in the SEAS during the winter monsoon [*Bruce et al.*, 1994; *Shankar and Shetye*, 1997]. The currents associated with these waves also bring in low-salinity waters from the northern BoB into the SEAS during November–January [*Shetye et al.*, 1991; *Rao and Sivakumar*, 2003]. Observations show that temperature inversions occur in the SEAS during November–February and that they propagate westward across the Lakshadweep Sea (LS; the part of the SEAS between the Indian west coast and the Lakshadweep islands: see Figure 1) along with the low-salinity waters from the BoB [*Shankar et al.*, 2003]. The inversions disappear by March, when the sea surface temperature (SST) increases along with the increase in surface heat fluxes into the LS. The inversions in the LS form in a barrier layer (BL; the layer between the base of the mixed layer and the top of the thermocline), which exists in climatologies for the SEAS [*Sprintall and Tomczak*, 1992; *Masson et al.*, 2002; *Rao and Sivakumar*, 2003]. The BL inhibits entrainment cooling of the mixed layer and traps the momentum transferred by the winds to the surface layer [*Vialard and Delecluse*, 1998]. *Shenoi et al.* [1999] hypothesised that the downwelling associated with the LH and the low-salinity surface layer provide a stable breeding ground for the SST high (SSTH) that forms in the LS in February–March, well before the large-scale heating due to surface fluxes leads to the formation of the warm pool in the SEAS prior to the summer monsoon [*Shenoi et al.*, 1999; *Rao and Sivakumar*, 1999]. The SSTH retains its identity even within the warm pool. Numerical simulations, however, show that the role of the ocean in the formation of the SSTH is not passive; the inversions present in the BL help heat the mixed layer above [*Durand et al.*, 2004], leading to an increase in SST. Since the "monsoon onset vortex" often forms over the warm SEAS [*Joseph*, 1990; *Rao and Sivakumar*, 1999], *Shenoi et al.* [1999] hypothesized that remotely forced ocean dynamics plays an important role in air-sea coupling in the SEAS by keeping the SST above 28°C, a rough threshold for deep atmospheric convection in the monsoon region [*Gadgil et al.*, 1984].

XBT observations show that the inversions in the LS initially decay in early March and disappear later, when the solar insolation increases [*Shankar et al.*, 2003]. We use CTD (Sea-Bird SBE 911Plus) data from time-series (TS) measurements made every two hours on board ORV Sagar Kanya at 74°30′E, 9°13′N in the LS (Figure 1) during 22-March–7-April and 23-May–7-June 2003 as part of the Arabian Sea Monsoon Experiment (ARMEX) to show that the disappearance of inversions owing to the increase in surface fluxes does not lead to the collapse of the BL, which persists till it is annihilated by remotely forced processes.

Barrier layer during March–June 2003

The inflow of low-salinity waters from the BoB into the LS first occurs in early December [*Shetye et al.*, 1991; *Shankar et al.*, 2003], when the westward Winter Monsoon Current (WMC) feeds into the poleward West India Coastal Current (WICC) [*Shankar et al.*, 2002]. In March, a low-salinity layer still occupies the top 80 m of the LS, the salinity in the top 20 m being 34.2–34.5 PSU (Figure 2). This low salinity at the surface creates a BL. The WICC reverses by February to flow equatorward off southwest India, but it still flows poleward along the rest of the west coast, where it reverses only in May [*Shankar et al.*, 2002]. This brings in waters of higher salinity at the surface (> 35.5 PSU) from the north [*Shetye et al.*, 1990] during May–June (Figure 2).

Following *Sprintall and Tomczak* [1992] and *Rao and Sivakumar* [2003], we define the mixed-layer depth (MLD) as the depth at which σ_t exceeds that at the surface by the increase in σ_t caused by a 1°C change in temperature. The depth of the top of the thermocline, herein referred to as the isothermal-layer depth (ILD), is defined as the depth at which temperature falls 1°C below SST. The thickness of the BL (BLT) is then the difference between ILD and MLD. The BLT can decrease (increase) if the MLD increases (decreases), or if the ILD decreases (increases), or if the MLD increases and ILD decreases (MLD decreases and ILD increases). Changes in ILD can be caused by upwelling or downwelling, and by changes in net surface heat flux; changes in MLD can be caused by air-sea fluxes of heat, precipitation and evaporation, mixing owing to the turbulent transfer of momentum from the winds, and the advection of heat and salt in the ML.

The BL is thicker during March-April (20 m on an average) than during May-June (< 5 m) (Figure 2). Though punctuated by three peaks (higher values) during March–April, the ILD shows a decreasing trend due to upwelling, which is evident in the temperature profiles; no such trend is

0094-8276/06/$5.00

seen in the MLD, which only shows two troughs (lower values). The first peak in ILD coincides with a trough in MLD and is due to a burst of fresher, cooler water in the ML during 27–29 March; this leads to a peak in the BLT. The second peak in ILD on 31 March coincides with an increase in MLD owing to a thickening of the surface low-salinity layer. This precedes the second burst of fresh water that shallows the MLD after 1 April; since the ILD increase and MLD decrease are out of phase this time, the BLT is not affected. Both ILD and MLD decrease after 31 March owing to a burst of fresh water and thinning of the low-salinity surface layer. The ML recovers to its mean value for the TS after the low-salinity plume is advected away from the TS location (TSL). The ILD recovers briefly to peak a third time during 2–3 April, as does the BLT, before both decline continuously till the end of the first TS on 7 April. The BLT collapses from 23 m early on 3 April to 7 m late on 6 April; 75% (25%) of this decrease in BLT is due to the decrease (increase) in ILD (MLD). In general,the BLT is affected more by changes in ILD than in MLD during March–April. This is also seen in the much higher correlation between the rates of change of ILD and BLT (0.741, significant at 99.99%) than between those of MLD and BLT (0.432, significant at 95%). (All correlations were computed for the filtered data shown in Figure 2 to avoid the effect of tides.)

The MLD is thicker during May–June than during March–April owing to an increase in net surface heat flux and the stronger winds (Figure 3); another factor is the increase in surface salinity and that this surface layer is thicker by 10 m compared to April. Upwelling persists during May–June and the ILD shows a decreasing trend. The MLD decreases slightly more than the ILD during 23–27 May owing to a decrease in the thickness of the surface low-salinity layer, and this results in a BLT increase from 7 m to 12 m. Immediately thereafter, early on 28 May, the MLD increases rapidly owing to an influx of high-salinity water and the BLT collapses below 5 m on 29 May. The BL does not recover after 29 May, and the ILD and MLD almost coincide thereafter. During this May-June TS, the BLT is affected almost equally by changes in ILD and MLD: the correlation between the rates of change of ILD and BLT (MLD and BLT) is 0.426 (0.450); both correlations are significant at 95%.

Discussion

We have shown that (i) a BL exists in the SEAS during March–April and May, (ii) the BL is thicker during March–April, when low salinities occur at the surface, (iii) it is almost annihilated by upwelling early in April, (iv) but recovers marginally in May, and (v) this relic BL is finally annihilated by the inflow of high-salinity waters in the surface layer from the north on 28 May.

The LH forms when a downwelling coastal Kelvin wave propagating poleward along the Indian west coast radiates offshore as a Rossby wave. When the high pinches off the coast, sea level falls towards the coast (see schematic in Figure 1) [*Shankar and Shetye*, 1997]; the sea-level fall and upwelling at the coast occur as early as February [*Sharma*, 1966; *Shankar and Shetye*, 1997]. This early onset of upwelling is also seen in 2003 in altimeter data, which show a near-continuous decrease in sea level from February–June (Figure 3); this upwelling in the SEAS occurs much before the large-scale cooling of the Arabian Sea with the onset of the summer monsoon in June [*Shenoi et al.*, 2002]. Surface salinity also increases continuously from March–June in the SEAS [*Han et al.*, 2001; *Shankar et al.*, 2003]. This implies that the processes seen during March–April and May–June continue unabated between the cruises, and are integral to the annual cycle in the SEAS, in which the LH is replaced by the Lakshadweep Low (LL) during the summer monsoon [*Shankar and Shetye*, 1997; *Schott and McCreary*, 2001].

Numerical simulations show that the LH and the associated early upwelling off southwest India are forced remotely by the winds that blow along the east coast of India [*McCreary et al.*, 1993; *Shankar and Shetye*, 1997; *Shankar et al.*, 2002]. Local forcing of upwelling starts much later in May [Figures 19 and 20 of *Shankar et al.*, 2002], and even then it is the cross-shore, not longshore, component at the coast that is strong in both climatological winds and QuikScat data. The winds measured by QuikScat (Figure 3) during 2003 at the coast or at the TSL (which are in good agreement with the winds measured on board) do not show any appreciable change before the upwelling burst during 3–7 April; the winds at this time are also much weaker than those during May–June, but the upwelling, as seen in the 30 m uplift of the 25°C isotherm during early April (Figure 2), is much stronger. Local Ekman pumping (Figure 3) causes sinking during 23-March–7-April (~ 3 m), with most of the sinking occurring after 28 March. This implies that the upwelling observed at TSL during March–April, which almost annihilates the BL, is forced not locally but remotely, as in the simulations of *Shankar et al.* [2002].

Local Ekman pumping causes negligible sinking (~ 0.2 m) during 23–28 May (Figure 3). Hence, the upwelling in late May is also remotely forced. Along the Indian west coast, salinity increases northward at the surface. High-salinity waters are brought into the SEAS by the equatorward WICC during April–October [*Shankar et al.*, 2002]; this current during May is due more to remote forcing than to local forcing.

The remote processes that force the SSTH during February start the previous October in the western BoB with the collapse of the summer monsoon [*Shenoi et al.*, 1999]; at this time, the LL still exists in the SEAS. The BL that exists in the LS as a consequence of the inflow of low-salinity waters from the BoB plays a major role in the formation and maintenance of the SSTH by inhibiting cooling of the warm surface layer by entrainment and by heating it from below when inversions exist in the BL [*Durand et al.*, 2004]. The data and arguments presented here show that the annihilation of the BL is also due primarily to processes that are forced remotely and are connected to the other half of the annual cycle in the LS, that of the LL. The upwelling that kills the BL starts in February, when the SSTH forms. The BL, however, survives till April, when it is almost annihilated by remotely-forced upwelling; the relic that survives is annihilated in May by the deepening of the ML due to the arrival of high-salinity waters from the north and the increase in wind speed.

Thus, the ARMEX data presented above show that the close link between the remotely forced ocean dynamics in the LS and its upper ocean thermodynamics leading to the formation of the SSTH also extends to the annihilation of the BL there. Later in June, the SST also falls below 28°C in the LS [*Reynolds and Smith*, 1994]. Since the ARMEX data end on 7 June, it is not possible to ascertain if the processes responsible for the annihilation of the BL also lead to the SST collapse. Numerical simulations are needed to examine this possibility.

Acknowledgments. Altimeter and QuikScat data were downloaded from the AVISO and SSMI websites; G .S. Bhat provided the wind data from ORV Sagar Kanya. R. Uchil and A. Mahale helped make the figures. This work was supported by DST and DOD, India. This is NIO contribution 3865.

References

Bruce, J. G., D. R. Johnson, and J. C. Kindle, Evidence for eddy formation in the eastern Arabian Sea during the northeast monsoon, *J. Geophys. Res.*, *99*, 7651–7664, 1994.

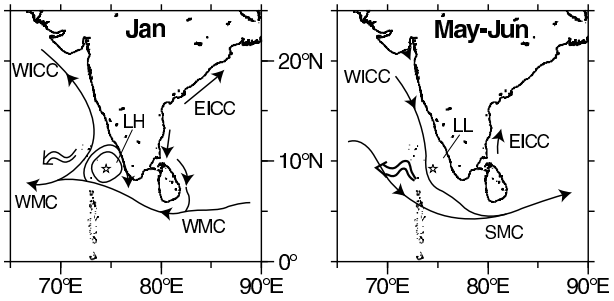

Figure 1. Schematic showing the evolution of the circulation in the LS during January (left) to June (right). The asterisk marks the TSL. The LH forms in January; the WMC flows around it. The WICC flows equatorward off southwest India, forcing coastal upwelling, but it flows poleward along the rest of the west coast. Westward radiation of Rossby waves is depicted by the wiggly arrow. The upwelling signal also propagates westward across the LS and the LL forms in May–June, when the WICC flows equatorward into the SMC (Summer Monsoon Current).

Durand, F., S. R. Shetye, J. Vialard, D. Shankar, S. S. C. Shenoi, C. Ethe, and G. Madec, Impact of temperature inversions on SST evolution in the southeastern Arabian Sea during the pre-summer monsoon season, *Geophys. Res. Lett.*, *31*, 10135, doi: 10.1029/2003GL18906, 2004.

Gadgil, S., P. Joseph, and N. Joshi, Ocean-atmosphere coupling over monsoon regions, *Nature*, *312*, 141–143, 1984.

Han, W., J. P. McCreary, and K. Kohler, Influence of precipitation minus evaporation and Bay of Bengal rivers on dynamics, thermodynamics, and mixed-layer physics in the upper Indian Ocean, *J. Geophys. Res.*, *106*, 6895–6916, 2001.

Joseph, P. V., Warm pool over the Indian Ocean and monsoon onset, *Tropical Ocean Atmos. News.*, *53*, 1–5, 1990.

Masson, S., P. Delecluse, J.-P. Boulanger, and C. Menkes, A model study of seasonal variability and formation mechanisms of the barrier layer in the eastern equatorial Indian Ocean, *J. Geophys. Res.*, *107*, 8017, doi:10.1029/2001JC000832, 2002.

McCreary, J. P., P. K. Kundu, and R. L. Molinari, A numerical investigation of the dynamics, thermodynamics and mixed-layer processes in the Indian Ocean, *Prog. Oceanogr.*, *31*, 181–244, 1993.

Rao, R. R., and R. Sivakumar, On the possible mechanisms of the evolution of a mini-warm pool during the pre-summer monsoon season and the onset vortex in the southeastern Arabian Sea, *Q. J. R. Met. Soc.*, *125*, 787–809, 1999.

Rao, R. R., and R. Sivakumar, Seasonal variability of sea surface salinity and salt budget of the mixed layer of the north Indian Ocean, *J. Geophys. Res.*, *108*, 3009, doi: 10.1029/2001JC000907, 2003.

Reynolds, R. W., and T. M. Smith, Improved global sea surface temperature analysis using optimum interpolation, *J. Clim.*, *7*, 929–948, 1994.

Schott, F., and J. P. McCreary, The monsoon circulation of the Indian Ocean, *Progr. Oceanogr.*, *51*, 1–123, 2001.

Shankar, D., and S. R. Shetye, On the dynamics of the Lakshadweep high and low in the southeastern Arabian Sea, *J. Geophys. Res.*, *102*, 12,551–12,562, 1997.

Shankar, D., P. N. Vinayachandran, and A. S. Unnikrishnan, The monsoon currents in the north Indian Ocean, *Progr. Oceanogr.*, *52*, 63–120, 2002.

Shankar, D., V. V. Gopalakrishna, S. S. C. Shenoi, S. R. Shetye, C. K. Rajan, J. Zacharia, N. Araligidad, and G. S. Michael, Observational evidence for westward propagation of temperature inversions in the southeastern Arabian Sea, paper presented at ARMEX workshop on data analysis and initial scientific results, Chennai, India, December 2003.

Sharma, G. S., Thermocline as an indicator of upwelling, *J. Mar. Biol. Assoc. India*, *8*, 8–19, 1966.

Shenoi, S. S. C., D. Shankar, and S. R. Shetye, On the sea surface temperature high in the Lakshadweep Sea before the onset of the southwest monsoon, *J. Geophys. Res.*, *104*, 15,703–15,712, 1999.

Shenoi, S. S. C., D. Shankar, and S. Shetye, Differences in heat budgets of the near-surface Arabian Sea and Bay of Bengal: Implications for the summer monsoon, *J. Geophys. Res.*, *107*, doi:10.1029/2000JC000679, 2002.

Shetye, S. R., A. D. Gouveia, S. S. C. Shenoi, D. Sundar, G. S. Michael, A. M. Almeida, and K. Santanam, Hydrography and circulation off the west coast of India during southwest monsoon, *J. Mar. Res.*, *48*, 359–378, 1990.

Shetye, S. R., A. D. Gouveia, S. S. C. Shenoi, G. S. Michael, D. Sundar, A. M. Almeida, and K. Santanam, The coastal current off western India during the northeast monsoon, *Deep-Sea Res.*, *38*, 1517–1529, 1991.

Sprintall, J., and M. Tomczak, Evidence of the barrier layer in the surface layer of the tropics, *J. Geophys. Res.*, *97*, 7305–7316, 1992.

Vialard, J., and P. Delecluse, An OGCM study for the TOGA decade. Part II: Barrier-layer formation and variability, *J. Phys. Oceanogr.*, *28*, 1089–1106, 1998.

S. S. C. Shenoi, D. Shankar, and S. R. Shetye, Physical Oceanography Division, National Institute of Oceanography, Dona Paula, Goa 403004, India (shenoi@darya.nio.org).

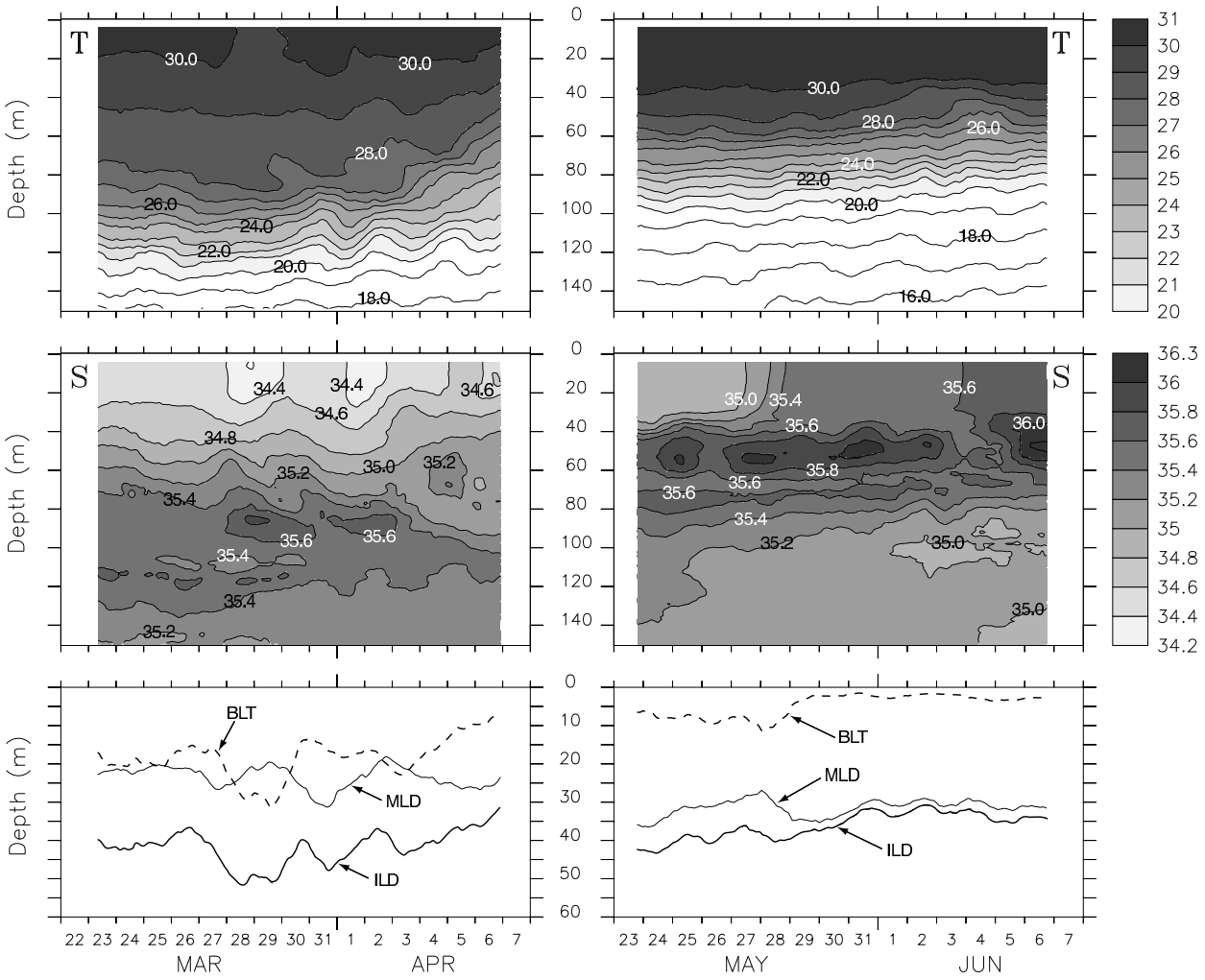

Figure 2. Time series during 22-March–7-April (left) and 23-May–7-June (right) at 74°30′E, 9°13′N in the LS of temperature (°C, top), salinity (PSU, middle), and isothermal-layer depth (ILD), mixed-layer depth (MLD), and barrier-layer thickness (BLT) (bottom). The measurements were made every two hours and have been filtered with a 25-hour running mean.

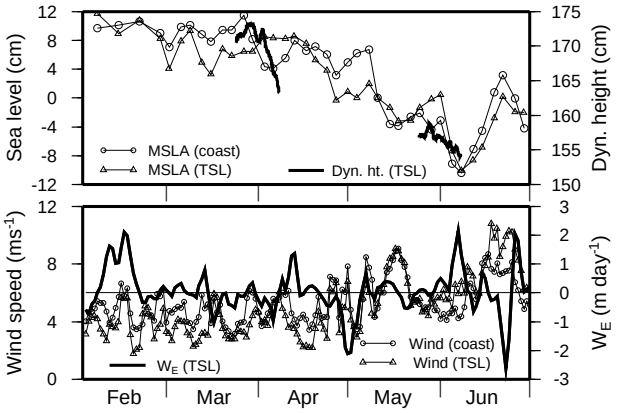

Figure 3. Satellite-based observations during February–June 2003. (Top) Altimeter mean-sea-level anomaly (MSLA, cm) at the coast and at TSL, and dynamic height (cm) computed from the TS data. (Bottom) Quikscat winds (m s^{-1}) at the coast and at TSL, and the Ekman pumping velocity (m day^{-1}) at TSL.